Int. J. Electrochem. Sci., 12 **(2017)** 11446 – 11454, doi: 10.20964/2017.12.71

International Journal of
ELECTROCHEMICAL
SCIENCE
www.electrochemsci.org

Short Communication

Preparation of High-Crystallinity and Large-Grain Br-doped Methylammonium Lead Iodide Thin Films at the Temperature Range of 100~140°C

Guannan Xiao, Chengwu Shi[*]*, Nannan Li, Long Li, Zhangpeng Shao*

School of Chemistry and Chemical Engineering, Anhui Province Key Laboratory of Advanced Catalytic Materials and Reaction Engineering, Hefei University of Technology, Hefei 230009, P. R. China
[*]E-mail: shicw506@foxmail.com, shicw506@hfut.edu.cn

Received: 16 August 2017 / *Accepted:* 29 September 2017 / *Published:* 12 November 2017

Br-doped methylammonium lead iodide ($CH_3NH_3PbI_{3-x}Br_x$) thin films with high crystallinity and large grain sizes were successfully obtained by converting a PbI_2·*N*-methyl-*2*-pyrrolidone (NMP) complex thin film using a conversion temperature and conversion time of 140 °C and 10 min, respectively. The influence of the conversion temperature on the crystal phase, morphology, optical absorption and chemical composition of the $CH_3NH_3PbI_{3-x}Br_x$ thin films was systematically investigated, and the photovoltaic performance of the corresponding planar perovskite solar cells was evaluated. The crystallinity of the $CH_3NH_3PbI_{3-x}Br_x$ thin films was enhanced, and their grain size gradually increased, with an increase in the conversion temperature from 100 °C to 120 °C to 140 °C. The planar perovskite solar cells based on films converted at 140 °C showed the best photoelectric conversion efficiency (PCE) of 13.56 %, with an open-circuit voltage (V_{oc}) of 1.01 V, a short-circuit photocurrent density (J_{sc}) of 18.90 mA·cm^{-2}, a fill factor (FF) of 0.71, and an average PCE of 12.46±1.10 %, with V_{oc} of 0.99 ± 0.03 V, J_{sc} of 18.31±1.16 mA·cm^{-2} and FF of 0.69 ± 0.04, all measured at a relative humidity of 50-54 % under illumination by simulated AM 1.5 sunlight (100 mA·cm^{-2}).

Keywords: Conversion temperature; Conversion time; PbI_2·NMP; $CH_3NH_3PbI_{3-x}Br_x$; Planar perovskite solar cell

1. INTRODUCTION

Organic-inorganic halide perovskite-based solar cells are recognized as one of the most promising candidates for solar energy harvesting due to their simple preparation [1-3] and substantial photoelectric conversion efficiency [4-6], and have rapidly turned into the focus of intensive academic

research and industrial interests in recent years. Fabricating high quality perovskite thin films with high crystallinity, large grain size and full-surface coverage is essential for enhancing the photovoltaic performance of perovskite solar cells; the quality of perovskite thin films is strongly affected by the conversion temperature. Burschka [7] were the first to utilize a conversion temperature and time of 70°C and 30 min, respectively, for conversion of a PbI_2 thin film by a sequential deposition method to obtain a methylammonium lead iodide ($CH_3NH_3PbI_3$) thin film albeit with a small grain size and poor coverage. The corresponding perovskite solar cells showed a photoelectric conversion efficiency (PCE) of 12.9 %. Boschloo [8] reported that the $CH_3NH_3PbI_3$ thin film can be prepared by a sequential deposition method using a conversion temperature of 100°C and conversion time of 20 min, with devices achieving a PCE of 13.5 %. Qiao [9] investigated the influence of different annealing temperatures ranging from 80 °C to 120 °C on the photovoltaic performance of $CH_3NH_3PbI_3$ solar cells and obtained the best PCE of 12.23 % at the annealing temperature and time of 120 °C and 20min. Seok [10] and Kim [11] increased the conversion temperature to 150 °C by intramolecular exchange to convert PbI_2·dimethylsulfoxide (DMSO) and PbI_2·*N*-methyl-*2*-pyrrolidone (NMP) complex thin films and prepared high-quality $FAPbI_3$ thin films, which were used to build devices with PCE of ~20 %. In our previous reports [12], a Br-doped methylammonium lead iodide ($CH_3NH_3PbI_{3-x}Br_x$) thin film with high crystallinity and full coverage was obtained by using a conversion temperature of 110°C and conversion time of 30 min, with the corresponding planar perovskite solar cells showing a PCE of 12.13 % at a relative humidity of 50-54 %. To the best of our knowledge, there has been little study of the influence of conversion temperature for the sequential deposition method on the crystal phase, morphology, optical absorption and chemical composition of $CH_3NH_3PbI_{3-x}Br_x$ thin films and on the photovoltaic performance in planar perovskite solar cells.

In this study, $CH_3NH_3PbI_{3-x}Br_x$ thin films with varying crystallinities, grain sizes and full coverage were successfully prepared by using conversion temperatures and times of 100 °C and 40 min, 120 °C and 20 min and 140 °C and 10 min, respectively. The influence of the conversion temperature and time on the crystal phase, morphology, optical absorption and chemical composition of $CH_3NH_3PbI_{3-x}Br_x$ thin films was investigated by X-ray diffraction (XRD), scanning electron microscopy (SEM), ultraviolet-visible-near infrared spectroscopy (UV-vis-NIR) and energy disperse spectroscopy (EDS), respectively. The influence of the conversion temperature and time on the photovoltaic performance of the corresponding planar perovskite solar cells was evaluated.

2. EXPERIMENTAL

Thin films of the 1.9 M PbI_2·NMP complex were prepared by spin-coating PbI_2·NMP complex precursor solution following our previous report [12]. The $CH_3NH_3PbI_{3-x}Br_x$ thin films were obtained by spin coating 100 μL of 0.535 M methylammonium halide mixture solution in isopropanol on top of the PbI_2·NMP thin films at 5000 rpm for 30 s, with a wait time of 30 s for drop casting before starting the spin coater [11]. The thin films were then placed onto a hot plate set to the conversion temperature (100 °C, 120 °C and 140 °C) inside a glove box with a relative humidity of 10-12 %. The

corresponding conversion times were 30 min, 40 min, and 50 min at 100 °C; 20 min, 30 min, and 40 min at 120 °C; and 10 min, 20 min, and 30 min at 140 °C.

The fabrication of perovskite solar cells including preparation of the 60-nm-thick TiO_2 compact layer, *spiro*-OMeTAD layer, 60-nm-thick gold electrode, characterization using XRD, FE-SEM, UV-vis-NIR, EDS and measurement of the photovoltaic performance followed our previous reports [13-15]. Black and opaque films on FTO were defined into individual addressable pixels with an active area of 0.09 cm^2 using a square aperture (3 mm × 3 mm). It is worth noting that the photoelectric conversion efficiency was measured in ambient atmosphere with a relative humidity of 50-54 %.

3. RESULTS AND DISCUSSION

3.1 Crystal phase and chemical composition of $CH_3NH_3PbI_{3-x}Br_x$ thin films

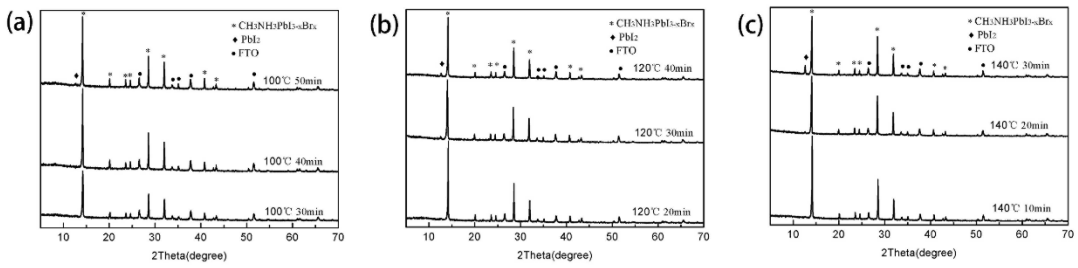

Figure 1. XRD patterns of $CH_3NH_3PbI_{3-x}Br_x$ thin films converted at a temperature of (a) 100 °C, (b) 120 °C and (c) 140 °C for different conversion times

Fig. 1 shows the XRD patterns recorded for $CH_3NH_3PbI_{3-x}Br_x$ thin films processed using a conversion temperature of 100 °C, 120 °C and 140 °C at different conversion times. The data show that the PbI_2·NMP complex thin films are converted into $CH_3NH_3PbI_{3-x}Br_x$ thin films at a conversion temperature of 100 °C and a conversion time of 30 min, 40 min and 50 min. When the conversion temperature was 100 °C, extension of the conversion time from 30 min to 40 min leads to an increase in the $CH_3NH_3PbI_{3-x}Br_x$ peak intensity at 2θ = 14.20° from 2413 to 4088. Further extension of the conversion time to 50 min leads to a decrease of the $CH_3NH_3PbI_{3-x}Br_x$ peak intensity at 2θ = 14.20° to 3616 and the appearance of a mild PbI_2 peak at 2θ = 12.70° [12-15]. These results indicate that the $CH_3NH_3PbI_{3-x}Br_x$ thin film shows poor crystallinity and decomposes to produce PbI_2 when the conversion time is extended to 50 min. The optimum conversion time at a conversion temperature of 100 °C was therefore 40 min, which shows an interesting difference in the preparation of perovskite thin films between two-step sequential deposition method and one-step spin-coating method [16]. When the conversion temperature was 120 °C, the $CH_3NH_3PbI_{3-x}Br_x$ peak intensity at 2θ = 14.20° was highest with a conversion time of 20 min compared to that at 30 min and 40 min, as shown in Fig. 1 (b). For the conversion time of 20 min, no PbI_2 peak was detected at 2θ = 12.70°. However, when the conversion time was extended from 20 min to 30 min to 40 min, the PbI_2 peak appears and gradually

strengthens. Therefore, the optimal conversion time at the conversion temperature of 120 °C was 20 min. Similarly, the optimal conversion time at the conversion temperature of 140 °C was determined to be 10 min, as shown in Fig. 1 (c).

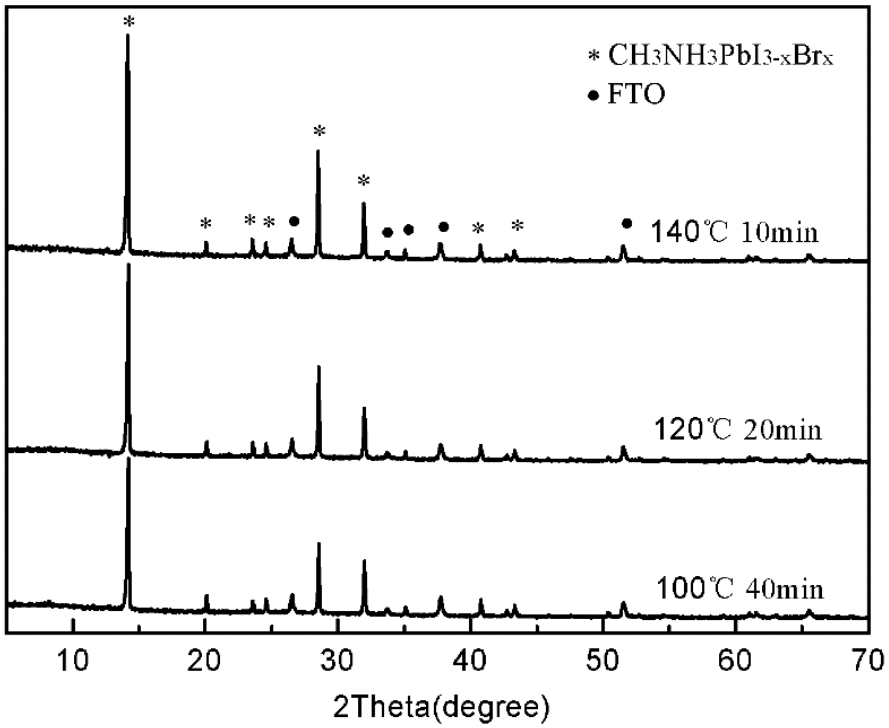

Figure 2. XRD patterns of $CH_3NH_3PbI_{3-x}Br_x$ thin films at a conversion temperature and optimum conversion time of (a) 100 °C and 40 min, (b) 120 °C and 20 min and (c) 140 °C and 10 min

Fig. 2 shows XRD patterns of $CH_3NH_3PbI_{3-x}Br_x$ thin films processed using a conversion temperature and optimum conversion time of 100 °C and 40 min, 120 °C and 20 min and 140 °C and 10 min. The diffraction peaks at 2θ = 14.20°, 20.10°, 23.57°, 24.61°, 28.57°, 31.98°, 40.79° and 43.33°correspond to the (110), (112), (211), (202), (220), (310), (224) and (330) reflection planes of $CH_3NH_3PbI_{3-x}Br_x$ with tetragonal perovskite structure [17-19], respectively, with a preferred orientation appearing along the (110) plane. No diffraction peaks corresponding to PbI_2 and PbI_2·NMP were detected, suggesting complete $CH_3NH_3PbI_{3-x}Br_x$ formation. Importantly, the $CH_3NH_3PbI_{3-x}Br_x$ peak intensity at 2θ = 14.20° increased with increasing conversion temperature from 100 °C to 120 °C to 140 °C. This result indicates that the crystallinity obtained for the $CH_3NH_3PbI_{3-x}Br_x$ thin film converted at a temperature of 140 °C was higher than that obtained at 100 °C and 120 °C. Table 1 shows the EDS results of $CH_3NH_3PbI_{3-x}Br_x$ thin films processed at a conversion temperature and optimum conversion time of 100 °C and 40 min, 120 °C and 20 min and 140 °C and 10 min. No obvious differences were found in the chemical composition of the $CH_3NH_3PbI_{3-x}Br_x$ thin films processed at different conversion temperatures and conversion times.

Table 1. EDS results of $CH_3NH_3PbI_{3-x}Br_x$ thin films processed at a conversion temperature and optimum conversion time of 100 °C and 40 min, 120 °C and 20 min and 140 °C and 10 min

Conversion temperature and optimum conversion time	Pb:I:Br
100 °C, 40 min	1:3.19:0.24
120 °C, 20 min	1:3.31:0.25
140 °C, 10 min	1:3.03:0.24

3.2 Surface morphology of $CH_3NH_3PbI_{3-x}Br_x$ thin films

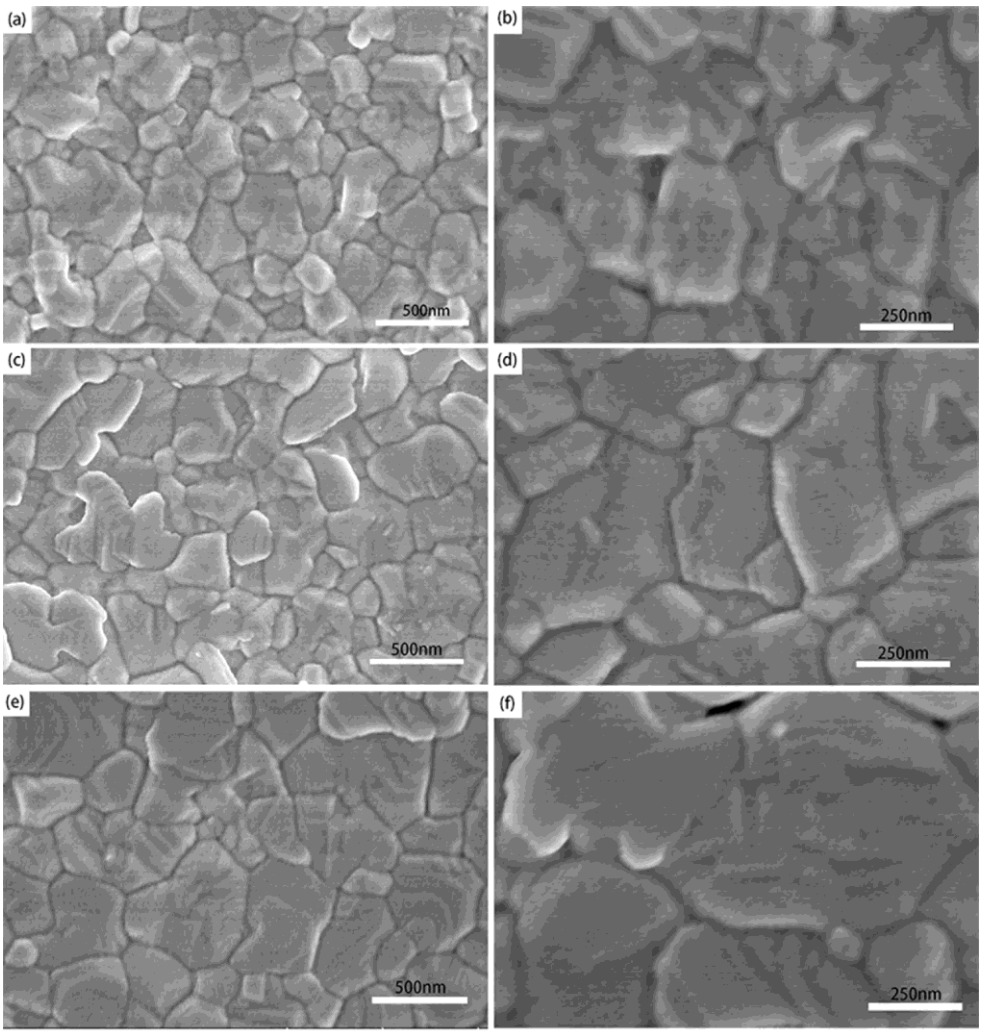

Figure 3. Surface SEM images of the $CH_3NH_3PbI_{3-x}Br_x$ thin films processed at a conversion temperature and optimum conversion time of (a,b) 100 °C and 40 min, (c,d) 120 °C and 20 min, and (e,f) 140 °C and 10 min

Fig. 3 shows the surface SEM images of the $CH_3NH_3PbI_{3-x}Br_x$ thin films processed at a conversion temperature and optimum conversion time of 100 °C and 40 min, 120 °C and 20 min and

140 °C and 10 min. On the one hand, the $CH_3NH_3PbI_{3-x}Br_x$ thin films converted at 100 °C, 120 °C and 140 °C all show a uniform and full coverage, with grain sizes of ~250 nm, ~500 nm and ~800 nm, respectively, which is beneficial for assembling efficient perovskite solar cells. On the other hand, this result demonstrates that the grain size gradually increases and the number of small grains decreases with increasing conversion temperature, which is conductive to the charge transporting in the $CH_3NH_3PbI_{3-x}Br_x$ thin film due to its decreasing intrinsic resistance. These data combined with the XRD results show that high-crystallinity, large-grain and full-coverage $CH_3NH_3PbI_{3-x}Br_x$ thin films can be successfully obtained by increasing the conversion temperature to 140 °C.

3.3 Absorption spectra of $CH_3NH_3PbI_{3-x}Br_x$ thin films

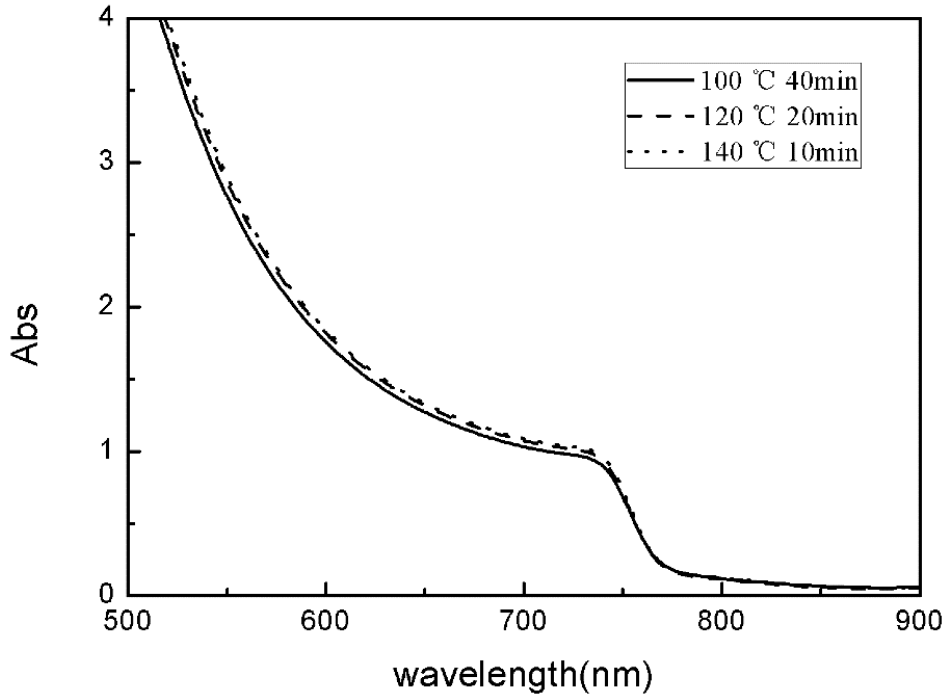

Figure 4. UV-vis-NIR absorption spectra of $CH_3NH_3PbI_{3-x}Br_x$ thin films processed at a conversion temperature and optimum conversion time of 100 °C and 40 min, 120 °C and 20 min and 140 °C and 10 min

Fig. 4 shows the UV-vis-NIR absorption spectra recorded for $CH_3NH_3PbI_{3-x}Br_x$ thin films. For all the films, the absorption onset is at a wavelength of 780 nm, with no obvious difference found in the measured absorbance from 550 nm to 850 nm for increasing conversion temperature from 100 °C to 120 °C to 140 °C. The result reveals that the high-crystallinity, large-grain and full-coverage $CH_3NH_3PbI_{3-x}Br_x$ thin film at the annealing temperature and the optimum annealing time of 140 °C and 10 min also exhibited the relative high absorbance in the range of 550-850 nm.

3.4 Photovoltaic performance of planar perovskite solar cells

Table 2. Photovoltaic performance parameters of planar perovskite solar cells

Conversion temperature and optimum conversion time		V_{oc} (V)	J_{sc} (mA·cm^{-2})	FF	η (%)
100 °C, 40 min	Best	0.98	18.58	0.65	11.78
	Average	0.96±0.03	17.62±0.96	0.66±0.03	11.23±0.92
120 °C, 20 min	Best	1.00	17.84	0.70	12.58
	Average	0.98±0.02	16.77±1.07	0.70±0.02	11.58±1.00
140 °C, 10 min	Best	1.01	18.90	0.71	13.56
	Average	0.99±0.03	18.31±1.16	0.69±0.04	12.46±1.10

*Average: 4 solar cells.

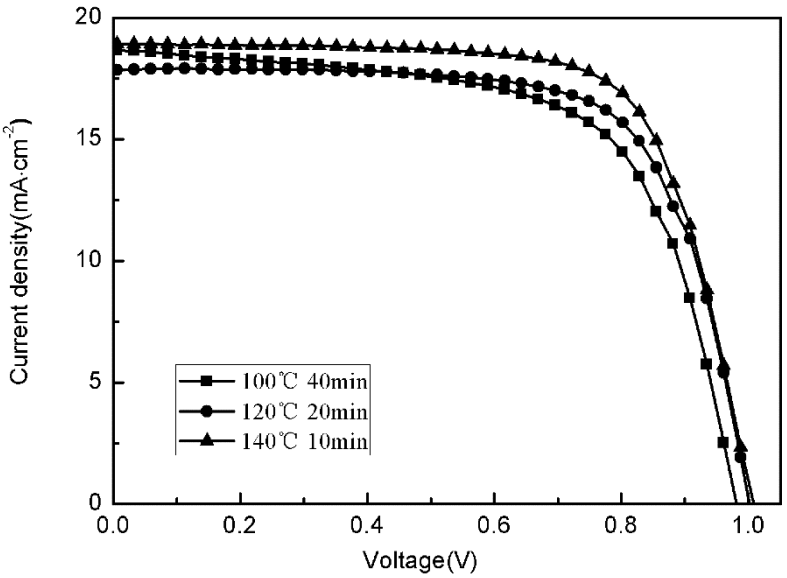

Figure 5. Photocurrent-photovoltage characteristics of planar perovskite solar cells

Fig. 5 shows the photocurrent versus photovoltage characteristics of planar perovskite solar cells, with the corresponding photovoltaic performance parameters listed in Table 2, and the definition of the photovoltaic performance parameters were described by the previous reports [20-21]. For increasing conversion temperature from 100 °C to 140 °C, the open-circuit voltage (V_{oc}) and fill factor (FF) increase from 0.96 ± 0.03 V and 0.66 ± 0.03 to 0.99 ± 0.03 V and 0.69 ± 0.04, respectively. These changes reflect the increased grain size and decreased number of grain boundaries in the $CH_3NH_3PbI_{3-x}Br_x$ thin films, which results in a decrease in the intrinsic resistance of the $CH_3NH_3PbI_{3-x}Br_x$ thin films. The short-circuit photocurrent density (J_{sc}) shows no significant change for increasing conversion temperature from 100 °C to 120 °C to 140 °C, consistent with the UV-vis-NIR data. Therefore, the planar perovskite solar cell fabricated by film conversion at a temperature of 140 °C shows the best PCE of 13.56 %, with V_{oc} of 1.01 V, J_{sc} of 18.90 mA·cm^{-2} and FF of 0.71; averaging over several devices gives a PCE of 12.46±1.10 %, V_{oc} of 0.99 ± 0.03 V, J_{sc} of 18.31±1.16 mA·cm^{-2}

and FF of 0.69 ± 0.04, all measured at a relative humidity of 50-54 % under the illumination of simulated AM 1.5 sunlight (100 $mA \cdot cm^{-2}$).

4. CONCLUSION

$CH_3NH_3PbI_{3-x}Br_x$ thin films with varying crystallinities, grain sizes and full coverage were successfully prepared by using a conversion temperature and optimum conversion time of 100 °C and 40 min, 120 °C and 20 min and 140 °C and 10 min, respectively. The results revealed that for increasing conversion temperature, the crystallinity and grain size of $CH_3NH_3PbI_{3-x}Br_x$ thin films is enhanced and gradually increased, respectively. Planar perovskite solar cells prepared by converting thin films at a temperature of 100 °C, 120 °C and 140 °C gave the best PCE of 11.78 %, 12.58 % and 13.56 % and the average PCE of 11.23±0.92 %, 11.58±1.00 % and 12.46±1.10 % (measured at a relative humidity of 50~54 % under illumination by simulated AM 1.5 sunlight, 100 $mA \cdot cm^{-2}$), respectively.

ACKNOWLEDGEMENTS
This work was financially supported by the National Natural Science Foundation of China (51472071, 51272061) and the Talent Project of Hefei University of Technology (75010-037004, 75010-037003).

COMPLIANCE WITH ETHICAL STANDARDS

CONFLICT OF INTEREST
The authors declare that they have no competing interests.

References

1. Y. Wang, S. Li, P. Zhang, D. Liu, X. Gu, H. Sarvari, Z. Ye, J. Wu, Z. Wang and Z. Chen, *Nanoscale*, 8 (2016) 19654.
2. N.J. Jeon, J.H. Noh, Y.C. Kim, W.S. Yang, S. Ryu and S.I. Seok, *Nat. Mater.*, 13 (2014) 897.
3. Q. Chen, H. Zhou, Z. Hong, S. Luo, H. Duan, H. Wang, Y. Liu, G. Li and Y. Yang, *J. Am. Chem. Soc.*, 13 (2014) 622.
4. A. Kojima, K. Teshima, Y. Shirai and T. Miyasaka, *J. Am. Chem. Soc.*, 131 (2009) 6050.
5. X. Dai, C. Shi, Y. Zhang and N. Wu, *J. Semicond.*, 36 (2015) 074003.
6. M. A. Green, K. Emery, Y. Hishikawa, W. Warta and E. D. Dunlop, *Prog. Photovolt. Res. Appl.*, 24 (2016) 3.
7. J. Burschka, N. Pellet, S.-J. Moon, R. Humphry-Baker, P. Gao, M.K. Nazeeruddin and M. Grätzel, *Nature*, 499 (2013) 316.
8. D. Bi, A.M. El-Zohry, A. Hagfeldt and G. Boschloo, *ACS Appl. Mater. Interfaces*, 6 (2014) 18751.
9. D. Khatiwada, S. Venkatesan, N. Adhikari, A. Dubey, A.F. Mitul, L. Mohammad, A. Iefanova, S.B. Darling and Q. Qiao, *J. Phys. Chem. C*, 119 (2015) 25747.
10. W.S. Yang, J.H. Noh, N.J. Jeon, Y.C. Kim, S. Ryu, J. Seo and S.I. Seok, *Science*, 348 (2015) 1234.

11. Y. Jo, K.S. Oh, M. Kim, K.–H. Kim, H. Lee, C.–W. Lee and D.S. Kim, *Adv. Mater. Interfaces* 3 (2016) 1500768.
12. N. Li, C. Shi, M. Lu, L. Li, G. Xiao and Y. Wang, *Superlattice. Microst.*, 100 (2016) 179.
13. J. Zhang, C. Shi, J. Chen, Y. Wang and M. Li, *J. Solid State Chem.*, 238 (2016) 223.
14. N. Wu, C. Shi, C. Ying, J. Zhang and M. Wang, *Appl. Surf. Sci.*, 357 (2015) 2372.
15. C. Ying, C. Shi, N. Wu, J. Zhang and M. Wang, *Nanoscale*, 7 (2015) 12092.
16. J. Qu, W. Wang, J. Cheng, S.Zhang, J. Ding and N. Yuan, *Int. J. Electrochem. Sci.*, 11 (2016) 10320.
17. M. Wang, C. Shi, J. Zhang, N. Wu and C. Ying, *J. Solid State Chem.*, 232 (2015) 20.
18. N. Li, C. Shi, Z. Zhang, Y. Wang, G. Xiao and R. Wang, *Opt. Mater.*, 60 (2016) 230.
19. J. Zhang, P. Barboux and T. Pauporté, *Adv. Energy Mater.*, 4 (2014) 1400932.
20. M. La, Y. Feng, C. Chen, C. Yang and S. Li, *Int. J. Electrochem. Sci.*, 10 (2015) 1563.
21. A. Sedghi and H. N. Miankushki, *Int. J. Electrochem. Sci.*, 10 (2015) 3354.